Meteorological Conditions Processing for Vision-based Traffic Monitoring

Nicolas Hautiere, Erwan Bigorgne, Jérémie Bossu, Didier Aubert

▶ To cite this version:

HAL Id: inria-00325657

https://inria.hal.science/inria-00325657

Submitted on 29 Sep 2008

Meteorological Conditions Processing for Vision-based Traffic Monitoring

Nicolas Hautière
LCPC - DESE
58 boulevard Lefebvre, 75015 Paris, France
nicolas.hautiere@lcpc.fr

Erwan Bigorgne
VIAMETRIS, Maison de la Technopole
6 rue Léonard de Vinci, 53000 Laval, France
erwan.bigorgne@viametris.fr

Jérémie Bossu
LCPC - DESE
58 boulevard Lefebvre, 75015 Paris, France
jeremie.bossu@lcpc.fr

Didier Aubert
LIVIC - INRETS/LCPC
14 route de la Minière, 78000 Versailles, France
didier.aubert@inrets.fr

Abstract

To monitor their networks, road operators equip them with cameras. Degraded meteorological conditions alter the transportation system operation by modifying the behavior of drivers and by reducing the operation range of the sensors. A vision-based traffic monitoring system is proposed to take fog and rain into account and react accordingly. A background modeling approach, based on a mixture of gaussians, is used to separate the foreground from the background. Since fog is steady weather, the background image is used to detect and quantify it and to restore the images. Since rain is a dynamic phenomenon, the foreground is used to detect it and rain streaks are removed from the images accordingly. The different detection algorithms are described and illustrated using actual images to show their potential benefits. The algorithms may be implemented in existing video-based traffic monitoring systems and allow the multiplication of applications running on roadside cameras.

1 Introduction

To monitor their networks, road operators equip them with networks of sensors, among which optical sensors, especially the cameras, are the most convenient. They are contact-less and can run multi-purpose applications: incident detection, wrong-way driver detection, traffic counting, etc. Degraded meteorological conditions alter the operation of the transport system in two ways. First, it is a cause of accidents. Second, the operation range of optical sensors is reduced. Hence, a vision-based traffic monitoring system must take adverse meteorological conditions into account and react accordingly. In other words, it must detect, quan-

tify and, if possible, mitigate the meteorological conditions so as to reduce the breakdown in the road transport system at its minimum value. This methodology has been followed so far for the problem of illumination assessment [33] and operation range assessment of optical sensors [22].

On the other hand, during the last decade, the problem of vision and adverse weather conditions has been largely tackled [26][19][13]. However, the integration of these works into operating surveillance systems has not been addressed so far. In this paper, a visual surveillance system is proposed which takes into account fog and rain. A background modeling approach is used to separate the foreground from the background in the video stream. Since fog is steady weather, the background image is used to detect and quantify it. Since rain is a dynamic phenomenon, the foreground is used to detect it. In this way, the proposed algorithms can be implemented in existing surveillance platforms.

2 Needs for Visibility Sensing

According to [1], the road visibility is defined as the horizontal visibility determined 1.2 m above the roadway. It may be reduced to less than 400 m by fog, precipitations or
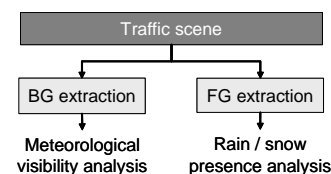

Figure 1. Principle of foreground (FG) and background (BG) models separation for weather conditions processing.
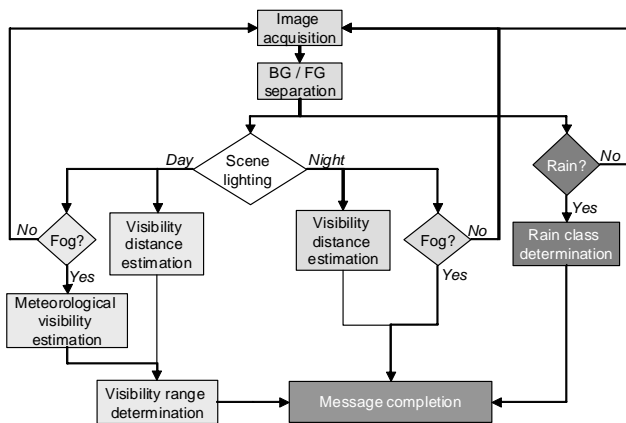
Figure 2. Camera-based RWIS architecture.

projections. Four visibility ranges are defined: <50, 50 to 100, 100 to 200 and 200 to 400. Based on these definitions, a visibility sensor should assign the visibility range to one of four categories and detect the origin of the visibility reduction, i.e. it should detect fog, rain and projections. These are adapted requirements for a Road Weather Information System (RWIS). In this paper, solutions are proposed to detect fog and daytime rain/snow, to estimate daytime fog density and to estimate the visibility range. However, the operation of optical sensors is altered by degraded weather conditions. Thus, there are also needs for mitigation solutions, which improve the operation range of existing outdoor vision-based applications. In this paper, solutions are proposed to mitigate the impact of daytime fog and rain.

3   System Overview

3.1   Principle

Common vision-based traffic monitoring systems rely on background modeling methods, where each video-frame is compared against a reference or background model to identify moving objects. Due to illumination changes and "long term" changes within the scene, it is necessary to constantly reestimate this background model. Thereafter, the time constants are generally set equal to the average time a moving object needs to cross the image. Adverse weather conditions have different temporal dynamics. Fog is generally considered as relatively steady weather, whereas rain or snow are dynamic phenomena. Based upon these considerations, the background model (BG) can thus be used to detect and estimate the fog density whereas the foreground model (FG) can be used to detect rain or snow presence. Once these phenomena have been detected and quantified, the resulting information can be used to generate recommendations to the drivers or to restore the images. This principle is summarized in Fig. 1.

3.2   Architectures

The detection of the weather conditions can be used either to generate warning messages or to restore the images accordingly. It leads to two different system architectures.

Camera-based RWIS   A first architecture of the system corresponds to a camera-based RWIS. Safety-related events are detected in the traffic scene and can be used to inform the driver by wireless communications or using a Variable Message Sign on the roadside. This solution is tested in the framework of the European project SAFESPOT [4]. First, BG and FG are extracted from the traffic scene. Second, a classification algorithm decides if it is daytime or nighttime. In each case, fog detection is performed and the visibility distance is estimated. In addition, if daytime fog is detected, the meteorological visibility distance, related to the fog density, is estimated. Finally, daytime rain detection is performed and a rain intensity class is determined. All this data is collected and is sent to the traffic center using an encoded message. The overview of this architecture is given in Fig. 2.

Pre-Processing Architecture   A second system architecture is a pre-processing software. Based on FG/BG separation, weather conditions are first estimated. If daytime fog is detected, the contrast of the image is restored with respect to the fog density. If rain is detected, the settings of the sensor are adjusted to reduce the visibility of rain in the images or rain streaks are removed from the FG model. Once the images are enhanced, they can be used by existing applications. This architecture is summarized in Fig. 3.
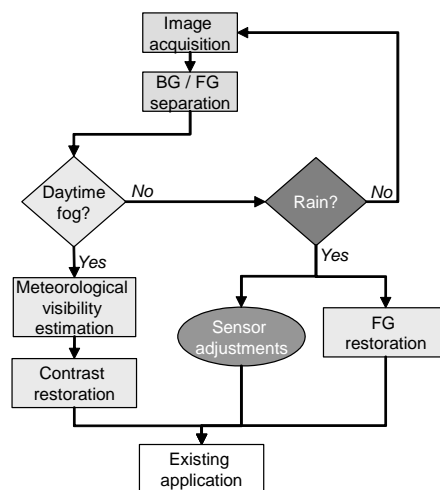

Figure 3. Pre-processing architecture.

In the following sections, the different software components are briefly described. The idea is to give an overview

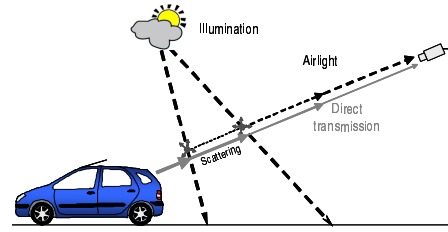**Figure 4. Foggy road scenes (a) in daytime and (b) in nighttime.**

Figure 5. Daytime fog: Light reflected by the object decreases with distance while skylight scattered by atmospheric particles increases with distance.

of each component and to see in particular how the BG/FG are used. The theoretical foundations, in particular the modeling of the visual effects of the meteorological phenomena, are given. Their relevant descriptors are given. References are cited for the technical details.

3.3 BG/FG Separation

The simplest form of background modeling is a time-averaged background image. This method suffers from many problems and requires a training period devoid of foreground objects. In addition, the approach cannot cope with gradual illumination changes in the scene. Due to illumination changes and "long term" changes within the scene, it is necessary to constantly update the background model. Many methods have been proposed to deal with these slowly-changing signals. Sparse methods compute the BG/FG models by using only the strong gradient edges. Dense methods compute the BG/FG using all the pixels. Sparse approaches are less sensitive to illumination changes, especially the approaches based on level sets computation [2]. Unfortunately, in our case, it is not possible to use such a method because the entire road surface (textureless) is required to feed the detection algorithms adequately (see next sections). A comparison of different dense methods is proposed in [7]. One of the best methods has been proposed by Grimson [32] and uses an adaptive Gaussian mixture (MoG) model per pixel. The implemented method is based on [32]. The differences lie in the update equations and the initialisation method, which are both described in [20]. Nevertheless, illumination changes may be problematic. They create artifacts in the BG model, so that the number of its edges suddenly increases. To overcome this problem, the number of edges is thus computed as well as its variations and a threshold is set above which the MoG must be initialized again. Another interesting improvement is proposed in [30] and should be tested.

4 Fog Processing

In this section, fog visual effects are first modeled. Second, detection methods are shown. Third, a mitigation method of daytime fog is proposed.

4.1 Visual Effects

Daytime Fog A sample image of a foggy road scene acquired by a roadside camera is given in Fig. 4(a). Daytime fog effects on light propagation are sketched in in Fig. 5. They were modeled by Koschmieder [24] who derived an equation relating the apparent luminance or radiance L of an object located at distance d to the intrinsic luminance L_0:

$$L = L_0 e^{-\beta d} + L_\infty (1 - e^{-\beta d}) \qquad (1)$$

where β is the extinction coefficient of the atmosphere and L_∞ is the atmospheric luminance. In the presence of fog, it corresponds to the luminance of the background sky. Duntley [24] developed a contrast attenuation law, stating that a nearby object exhibiting contrast C_0 with the background will be perceived at distance d with the following contrast:

$$C = [L - L_f / L_\infty] e^{-\beta d} = C_0 e^{-\beta d} \qquad (2)$$

This expression stands as a basis for the definition of a standard dimension called "meteorological visibility distance" V_{met}, i.e. the greatest distance at which a black object (C_0=-1) of a suitable dimension can be seen in the sky on the horizon, with the threshold contrast set at 5% [8]:

$$V_{met} = -\ln(0.05)/\beta \approx 3/\beta \qquad (3)$$

Nighttime Fog Another sample image of a foggy road scene acquired by a roadside camera is given in Fig. 4(b). Nighttime fog effects are sketched in Fig.6. The luminous range is the greatest distance at which a given light signal can be recognized in any particular circumstances, as limited only by the atmospheric transmissivity and by the threshold of illuminance at the eye of the observer [8]. It can be put in relation to Allard's law relating the illuminance E produced on a surface by a light source to the luminous intensity I_L of the source in the direction of the surface, to the distance d between the surface and the source, and the extinction coefficient of the atmosphere β. The surface is
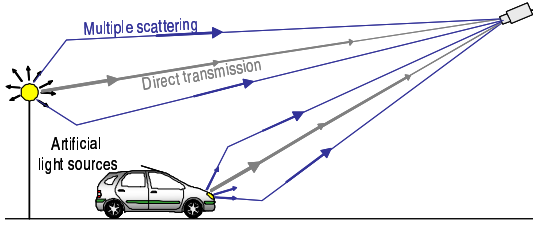
Figure 6. Nighttime fog: The direct transmission of artificial light sources decreases with distance. Multiple scattering creates halos around them.
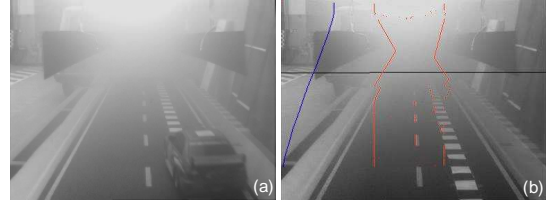

Figure 7. Daytime fog detection: (a) original daytime video sequence; (b) black line: meteorological visibility distance estimation; blue curve: instantiation of (6); red lines: limits of the vertical band analyzed.

normal to the direction of the source and sufficiently distant for the source to be considered as a point source:

$$E = (I_L/d^2)e^{-\beta d} \tag{4}$$

Light scattering creates also halos or glows around artificial light sources. These halos are affected by two parameters: the phase function of particles and the extinction coefficient β of the atmosphere. [11] shows that this phenomenon is similar to a convolution. Assuming a specific phase function [27] proposes an analytical model of halos based on Legendre polynomia. [23] proposes to use Generalized Gaussian Distributions to approximate this solution.

4.2 Detection and Quantification

Since visual effects of fog differ between daytime and nighttime, fog detection is performed differently in each condition.

Daytime Fog Assuming that the road is locally planar, the distance of a point located at the range d on the road can be expressed using a pinhole camera model by:

$$d = \lambda/(v-v_h) \tag{5}$$

where $\lambda = \frac{H\alpha}{\cos^2(\theta)}$ and $v_h = v_0 - \alpha \tan(\theta)$. θ denotes the pitch angle of the camera, while v_h represents the vertical position of the horizon line in the image. The intrinsic parameters of the camera are its focal length f, and the size t_p of a pixel. We have also made use herein of $\alpha = \frac{f}{t_p}$. H denotes the sensor mounting height. In a foggy image, the intensity I of a pixel is the result of the camera response function crf [14] applied to (1). Assuming that crf is linear, (1) becomes:

$$I = \text{crf}(L) = Re^{-\beta d} + A_\infty(1 - e^{-\beta d}) \tag{6}$$

where R is the intrinsic intensity of the pixel, i.e. the intensity corresponding to the intrinsic luminance value of the corresponding scene point and A_∞ is the background sky

intensity. After a change of d according to v (5), one obtains β by taking the second derivative of I with respect to v:

$$\partial^2 I/\partial v^2 = 0 \iff \beta = 2(v_i-v_h)/\lambda \tag{7}$$

where v_i denotes the position of the inflection point of $I(v)$. V_{met} is deduced using (3). An implementation of this principle is proposed in [19]. A sample result is given in Fig. 7.

Night Fog Night fog situation has been tackled in [26]. Authors compute the 3-D positions of light sources based on two different images of the same place acquired under two different weather conditions. They have a linearly calibrated camera and rely on Allard's law (4). Conversely, assuming two similar light sources placed at two distances d_1 and d_2, β can be approximated by:

$$\beta = [1/(d_2-d_1)]\ln(I_1/I_2) \tag{8}$$

where I_1 and I_2 denote the image brightness values of the light sources in the image. However, such a linearly calibration is not realistic because it leads to non saturated light sources. If the light sources are not saturated, traffic monitoring will be inoperative since the darker road surface is under-exposed. Since (8) is not easy to implement, the halos remain to test. It is proposed to detect light sources in the BG model and to estimate the profile of the halo. In this aim, ellipses are fitted along the level lines [12] and the halo profile estimated using the main axis of the ellipse. This principle is shown in Figs.8(a)(b). In the absence of fog, the halo profiles are abrupt on both close and distant light sources. In the presence of fog, the halo profiles are smooth on close light sources and abrupt on distant light sources due to the dominating attenuation effect. By computing the area S between the halo profiles $I_h(R)$ of distant and close light sources, night fog can thus be detected:

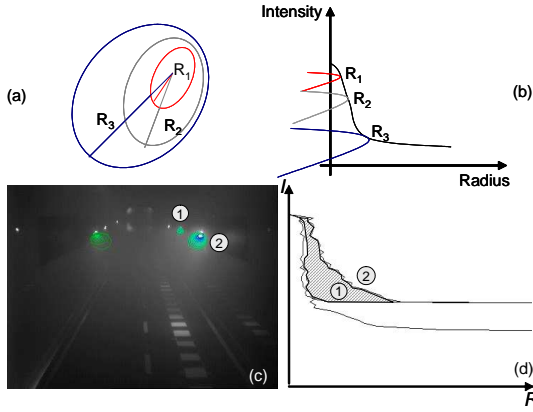$$S = \int \Big[I_{h_1}(R) - I_{h_2}(R)\Big]\mathrm{d}R \tag{9}$$

Figure 8. Night fog detection: (a)(b) process to estimate the halo profiles by fitting ellipses; (c) fitted ellipses on a sample image; (d) halo profiles and area S (9) in gray.
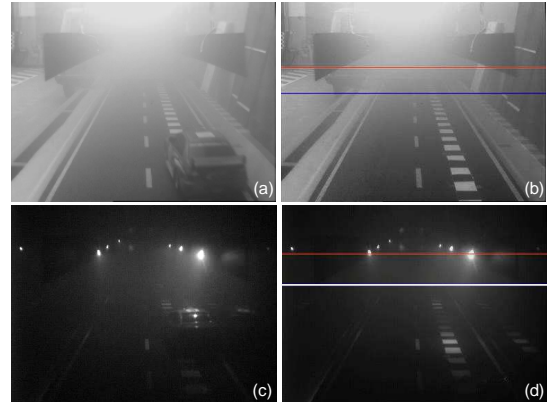

Figure 9. Visibility distance estimation: (a)(c) original daytime and nighttime videos; (b)(d) visibility distance estimations depicted by the lowest horizontal lines.

This method has been prototyped and a sample result is given in Fig. 8. Fig. 8(c) shows the detection and the fitting of halos around artificial light sources. Fig. 8(d) gives the estimated halo profiles around the main axes of the fitted ellipses. The area S, given by (9), between the profile of the close light source (source 2) and the furthest one (source 1) is marked in gray. According to [27, 23], the halo profiles may be also used to estimate the extinction coefficient β and the phase function of the atmosphere. In these papers, authors use images acquired with a high-resolution camera device [28]. In our tests (see section 6) obtained with a low cost CCD camera, it seems difficult to fit the proposed halo models. This is however good perspectives for our work.

4.3 Estimation of the Visibility Distance

The previous methods detect that the visibility is reduced by fog and, if possible, estimate its density. However, the same fog density in daytime or in nighttime does not reduce the road visibility in the same way. A generic method is thus needed to estimate the actual visibility distance. To perform this task, methods are already proposed in the literature. [5] computes the highest edge in the image having a contrast above 5% using a wavelet transform. [15] proposed a Weighted Intensity Power Spectra (WIPS) algorithm. [16] proposed an algorithm which examines edges within the image and performs a comparison of each image with a historical composite image. However, they do not take into account the 3-D structure of the scene to compute their visibility distance. The methods are thus sensitive to the presence of moving objects in the scene.

Based on these methods, a method is proposed which consists in computing the distance corresponding to the highest visible point in the driving space area in the BG model. In this way, the method is not sensitive to the presence of moving objects in the scene.

The driving space area is obtained by computing a temporal accumulation of the FG model. The detection of the visible edges in the BG model is performed by a technique based on the Contrast Sensitivity Function (CSF) of a human eye [6]. For each 8×8 block of pixels, the algebraic area $\bar{A}$ between its spectrum B obtained by a DCT and CSF^{-1} is computed:

$$\bar{A} = \int_{\mathbb{R}_+^*} \Big[B(f) - CSF^{-1}(f) \Big] \, \mathrm{d}f \qquad (10)$$

A threshold on $\bar{A}$ is then set to decide wether an edge is visible or not in the considered block of pixels [17]. In this aim, the latter is set, so that the set of visible edges using daytime acquired images are the edges having at least 5% of contrast. In this way, the edges having at least 5% of contrast are detected by daytime, which is less computational demanding, and the above described approach is used by nighttime.

4.4 Daytime Fog Mitigation

To restore the contrast, it is proposed to reverse (6), which becomes:

$$R = Ie^{\beta d} + A_\infty (1 - e^{\beta d}) \qquad (11)$$

Thanks to 4.2, (β, A_∞) can be recovered. Therefore, the remaining problem is the estimation of the depth d of the pixels. [18] shows a depth heuristic which is relevant for traffic applications. It is decomposed in three parts: the road surface, the sky and the surroundings. The depth d of a pixel at coordinates (u, v) which does not belong to the
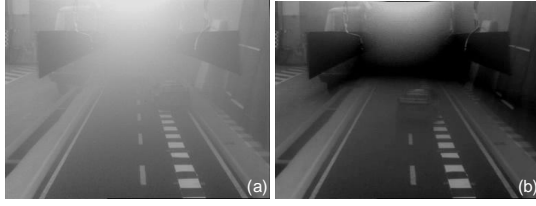
Figure 10. Daytime fog mitigation: (a) original image; (b) contrast restored image.

Figure 11. (a) Original rainy image; (b) BG model; (c) FG model; (d) resulted rain streaks.

sky region, i.e. whose intensity is lower than A_∞ is given by:

$$d = \min(d_1, d_2) \qquad (12)$$

where d_1 models the depth of pixels belonging to the road surface and is given by (5). d_2 models the depth of verticals objects:

$$d_2 = \kappa/(u - u_h) \qquad (13)$$

In these equations, (u_h, v_h) denotes the vanishing point position in the image, λ depends on the intrinsic and extrinsic camera parameters and $\kappa > \lambda$ controls the relative importance of the vertical world with respect to the flat world. Finally, a clipping plane at $d = \lambda/(c - v_h)$ is used to limit the depth modeling errors near the horizon line. In [18], in-vehicle methods are proposed to adjust automatically these model scene parameters. In the context of a fixed camera, the scene parameters can be set empirically, like in [25].

5 Hydrometeors Processing

5.1 Visual Effects

The constituent particles, called the hydrometeors, of dynamic weather conditions such as rain, snow and hail are larger than in fog and individual particles may be visible in the image. A set of such drops falling at high velocities results in time varying intensity fluctuations in images and videos. In addition, due to the settings of the camera used to acquire the images, intensities due to rain are motion blurred and therefore depend on the background. Thus, the visual effects of rain are a combined effect of the dynamics of rain and the photometry of the environment. Stochastic models that capture the spatial and temporal effects of rain are proposed in [13].

5.2 Detection and Quantification

[13] proposes a local method to detect rain streaks in images, which relies on two constraints. First, the intensities I_{n-1} and I_{n+1} must be equal and the change in intensity

due to a hydrometeor in the nth frame satisfies the constraint:

$$\Delta I = I_n - I_{n-1} = I_n - I_{n+1} \geq c \qquad (14)$$

where c is a threshold that represents the minimum change in intensity due to a rain drop. Then, they retain the pixel if the intensity change ΔI is linearly related to the background intensity I_{n-1}. Second, they search a temporal correlation in the rain streaks between neighboring pixels in the direction of rain. Another approach is proposed in [3] which uses global frequency information to remove rain and snow in image space.

Once camera parameters are adjusted to see rain, background substraction can be used to extract rain streaks from traffic videos. Indeed, they can be considered as outliers of the MoG. Figs. 11(a)&(b) shows a rainy image and its corresponding BG model. Fig 11(c) shows the FG model, where rain streaks are visible. However, other objects are present in it. Using a floodfill algorithm, large objects can be filtered. Then, the constraint (14) is applied. However, instead of comparing successive images, we check that the pixels in the filtered FG image have an intensity greater than the BG image, what gives similar results. Thereafter, only rain streaks combined with noisy features remain (see Fig. 11(d)). To filter the latter, rain streaks are assumed to be majority and to be almost vertically oriented. The gradients orientation is then computed on the rain streaks using Canny-Deriche filter [10] and assigned to a category [2]. A cumulative histogram is then computed.

The remaining task is thus to detect an eventual peak in the histogram which can be related to the rain/snow intensity. In a first approximation, it is modeled as a normal distribution. A χ^2 test is thus performed to check this assumption. A sample result of histogram and normal law fitting is

proposed in Fig. 12(a). In this figure, the peak corresponding to the rain intensity is high. It can thus be deemed that rain or snow is falling.

If the χ^2 test is negative, a bimodal distribution is assumed, where the second part of the histogram contains the orientation of noisy pixels. The latter come from small objects which remained after the filtering of the FG model. They should theoretically not have major orientations, and so they could thus be modeled as a uniform distribution. The complete bimodal histogram is thus modeled as a uniform-normal mixture model whose parameters can be estimated using an EM algorithm [9]. However, in structured scenes, such as urban areas, the orientations of the noisy features are not random. In particular, the horizontal noisy features are quite numerous. Consequently, the use of two normal laws proves to be also relevant and is faster to solve using Otsu's algorithm for example [29]. Additional work is still needed to validate the approach.

5.3   Mitigation

[13] proposed to adjust the settings (lens aperture, exposure time) of a camera to reduce the visibility of rain streaks in images. In camera-based surveillance systems, the settings of the cameras are either fixed or automatically varied using an auto-iris lens. Instead of reducing the visibility of rain streaks in the images, an alternate process is to remove them from the BG model. In the previous paragraph, rain orientation was obtained thanks to a global information on the gradients orientation in the FG model. To remove rain streaks, a local but robust method must be used to estimate the orientation of the pixel blobs. In this aim, the geometrical moments of the blobs are computed and their orientation is deduced [31]. The blobs with an orientation corresponding to the rain one are considered as rain components and are removed from the FG model. Following this principle, the rain streaks are put in green in Fig. 12(b) and the other moving objects are put in red.
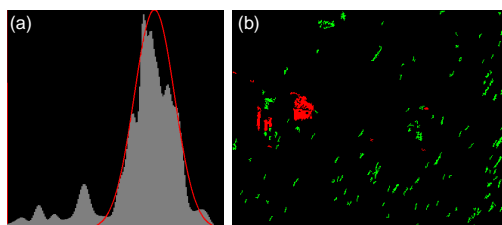

Figure 12. (a) Histogram of gradients orientation of the rain streaks and fitting of a normal law; (b) Mitigation of the rain in the FG model by filtering of the rain drops.

6   Experimental Results

The experimental results in this paper are not numerous. They are rather used to illustrate the potential of analyzing separately the BG and FG models in order to estimate the environmental conditions.

Fog   Currently, we do not have video sequences of fog acquired by a roadside camera. Existing video databases [21] do not fulfill our requirements since the horizon line is not visible. Consequently, the described system, summarized in Figs. 2&3, has only been tested on a reduced scale model using a glass tank in which some scattering medium is injected using a fog machine. The sun is replaced by two strong light projectors. The sky is replaced by some scattering material put on the roof of the aquarium. For night tests, powerful LEDs are used to simulate a public lighting installation. Remote control cars are used to create road traffic. The original video sequences with a moving car inside the tank are illustrated in Figs. 7(a) and 9(c). Meteorological visibility estimation is shown in Fig. 7(b). Night fog detection is shown in Figs. 8(c)&(d). Visibility distance estimation is shown in Figs. 9(b)&(d). Finally, contrast restoration is shown in Fig. 10.

Hydrometeors   The results concerning the processing of hydrometeors are obtained using a challenging video sequence in an urban context with a lot of moving objects. This video is illustrated in Fig. 11(a). Results are given in Fig. 11(b)(c)&(d) and Fig. 12.

7   Conclusion

In this paper, a scheme is proposed which consists in processing the environmental conditions using outdoor video cameras. A first architecture of the system corresponds to a camera-based RWIS and can be used to warn the drivers about inclement weather conditions. A second architecture of the system corresponds to a pre-processing architecture which enables to mitigate the impact of weather conditions on the operation of surveillance applications. The different components are described. A MoG is used to separate the foreground from the background in current images. Since fog is a steady weather, the background image is used to detect and quantify it. Since rain is a dynamic phenomenon, the foreground is used to detect it. In this way, the proposed algorithms can be implemented in existing surveillance platforms without revising the system architecture. Methods to detect, quantify and mitigate fog and rain are presented and illustrated using actual images. An additional method is used to estimate the visibility range. All these methods rely on the modeling of visual effects of rain and

fog. In a close future, the technical validation of these methods and their integration in the SAFESPOT project applications is foreseen.

Acknowledgments

References

[1] AFNOR. Road meteorology - gathering of meteorological and road data - terminology. NF P 99-320, April 1998.

[2] D. Aubert, F. Guichard, and S. Bouchafa. Time-scale change detection applied to real time abnormal stationarity monitoring. *Real-Time Imaging*, 10(1):9–22, 2004.

[3] P. Barnum, T. Kanade, and S. Narasimhan. Spatio-temporal frequency analysis for removing rain and snow from videos. In *International Workshop on Photometric Analysis For Computer Vision*, 2007.

[4] R. Brignolo, L. Andreone, and G. Burzio. The SAFESPOT Integrated Project: Co-operative systems for road safety. In *Transport Research Arena*, 2006.

[5] C. Bush and E. Debes. Wavelet transform for analyzing fog visibility. *IEEE Intelligent Systems*, 13(6):66–71, November/December 1998.

[6] F. W. Campbell and J. G. Robson. Application of fourier analysis to the visibiliy of gratings. *Journal of Physiology*, pages 551–566, 1968.

[7] S.-C. Cheung and C. Kamath. Robust techniques for background subtraction in urban traffic video. In *Video Communications and Image Processing, SPIE Electronic Imaging*, pages 881–892, 2004.

[8] CIE. *International Lighting Vocabulary*. Number 17.4. 1987.

[9] N. Dean and A. Raftery. Normal uniform mixture differential gene expression detection for cDNA microarrays. *BMC Bioinformatics*, 6(173), 2005.

[10] R. Deriche. Using canny's criteria to derive an optimal edge detector recursively implemented. *International Journal of Computer Vision*, 2(1):167–187, April 1987.

[11] E. Dumont and V. Cavallo. Extended photometric model of fog effects on road vision. *Transport Research Records*, (1862):77–81, 2004.

[12] A. Fitzgibbon, M. Pilu, and R. Fisher. Direct least-squares fitting of ellipses. *IEEE Transactions on Pattern Analysis and Machine Intelligence*, 21(5):476–480, May 1999.

[13] K. Garg and S. Nayar. Vision and rain. *International Journal of Computer Vision*, 75(1):3–27, October 2007.

[14] M. Grossberg and S. Nayar. Modelling the space of camera response functions. *IEEE Transactions on Pattern Analysis and Machine Intelligence*, 26(10):1272–1282, 2004.

[15] T. Hagiwara, Y. Ota, Y. Kaneda, Y. Nagata, and K. Araki. A method of processing CCTV digital images for poor visibility identification. *Transportation Research Records*, 1973:95–104, 2007.

[16] R. Hallowell, M. Matthews, and P. Pisano. An automated visibility detection algorithm utilizing camera imagery. In *AMS Annual Meeting*, 2007.

[17] N. Hautière and D. Aubert. Visible edges thresholding: a HVS based approach. In *Proc. Int. Conf. on Pattern Recognition*, volume 2, pages 155–158, 2006.

[18] N. Hautière, J.-P. Tarel, and D. Aubert. Towards fog-free in-vehicle vision systems through contrast restoration. In *Proc. IEEE Computer Vision and Pattern Recognition*, 2007.

[19] N. Hautière, J.-P. Tarel, J. Lavenant, and D. Aubert. Automatic fog detection and estimation of visibility distance through use of an onboard camera. *Machine Vision Applications*, 17(1):8–20, 2006.

[20] P. KadewTraKuPong and R. Bowden. An improved adaptive background mixture model for real-time tracking with shadow detection. In *European Workshop on Advanced Video-Based Surveillance Systems*, 2001.

[21] K. U. Karlsruhe. Traffic image sequences and 'marbled block' sequence. http://i21www.ira.uka.de/.

[22] R. Kurata, H. Watanabe, M. Tohno, T. Ishii, and H. Oouchi. Evaluation of the detection characteristics of road sensors under poor-visibility conditions. In *IEEE Intelligent Vehicles Symposium*, 2004.

[23] S. Metari and F. Deschênes. A new convolution kernel for atmospheric point spread function applied to computer vision. In *Proc. IEEE Int. Conf. Computer Vision*, October 2007.

[24] W. Middleton. *Vision through the atmosphere*. University of Toronto Press, 1952.

[25] S. G. Narashiman and S. K. Nayar. Interactive deweathering of an image using physical model. In *IEEE Workshop on Color and Photometric Methods in Computer Vision*, 2003.

[26] S. G. Narasimhan and S. K. Nayar. Vision and the atmosphere. *Int J Comput Vis*, 48(3):233–254, 2002.

[27] S. G. Narasimhan and S. K. Nayar. Shedding light on the weather. In *IEEE Conference on Computer Vision and Pattern Recognition*, 2003.

[28] S. G. Narasimhan, C. Wang, and S. Nayar. All the images of an outdoor scene. In *Proc. European Conf. Computer Vision*, volume 3, pages 148–162, 2002.

[29] N. Otsu. A threshold selection method from graylevel histogram. *IEEE Transactions on Systems, Man and Cybernetics*, 1(9):62–69, 1979.

[30] C. Poppe, G. Martens, P. Lambert, and R. Van de Walle. Improved background mixture models for video surveillance applications. In *Proc. Asian Conf. Computer Vision*, 2007.

[31] R. Safee-Rad, K. Smith, B. Benhabib, and I. Tchoukanov. Application of moment and fourier descriptors to the accurate estimation of elliptical-shape parameters. *Pattern Recognition Letters*, 13(7):497–508, 1992.

[32] C. Stauffer and W. Grimson. Learning patterns of activity using real-time tracking. *IEEE Transactions on Pattern Analysis and Machine Intelligence*, 22(8):747–757, 2000.

[33] L. Wixson, K. Hanna, and D. Mishra. Improved illumination assessment for vision-based traffic monitoring. In *IEEE International Workshop on Visual Surveillance*, volume 2, pages 34–41, 1998.